SEPTEMBER 1982 211/82

NUMERICAL ANALYSIS OF AN OPTICALLY PUMPED D_2O FIR LASER

T. Okada, R. Behn, M.A. Dupertuis,
P.D. Morgan, M.R. Siegrist

NUMERICAL ANALYSIS OF AN OPTICALLY PUMPED D_2O FIR LASER

T. Okada*, R. Behn, M.A. Dupertuis,

P.D. Morgan+, M.R. Siegrist

Centre de Recherches en Physique des Plasmas

Association Euratom - Confédération Suisse

Ecole Polytechnique Fédérale de Lausanne

CH-1007 Lausanne / Switzerland

* present address: Department of Energy Conversion,

Graduate School of Engineering Sciences,

Kyushu University, 33 Kasuga,

Fukuoka 816, Japan

+ present address: JET Joint Undertaking

Abingdon, Oxfordshire OX14 2EA

England

ABSTRACT

The performance of a pulsed D_2O laser pumped longitudinally by a CO_2 laser and emitting at 385 microns is investigated numerically. These studies point out the limitations in pumping efficiency due to the "bottle-neck" effect in the vibrational deexcitation of D_2O. The influence of a buffer gas on the saturation behaviour is discussed. The results of this numerical simulation are in good agreement with experimental measurements. Design parameters are predicted for a D_2O laser system suitable for Thomson scattering diagnostics of a Tokamak plasma.

I. INTRODUCTION

Extensive studies are currently in progress to develop high-power optically pumped FIR lasers for Thomson scattering measurements in Tokamak plasmas [1]. In order to achieve a good signal to noise ratio during heterodyne detection of the scattered radiation, high power laser pulses with microsecond pulse duration are required. Up to now most of the experiments reported are limited to short pulse operation with pulses of the order of 100 nsec. In CO_2-laser-pumped D_2O lasers, the most promising system developed so far, it is difficult to achieve long pulses at high powers mainly because of the slow decay time of the excited vibrational manifold. This so-called bottleneck effect is mainly responsible for poor efficiency and leads to the requirement of a large active volume [2]. Hence, it is important to simulate the operational characteristics, in order to optimize the design and to improve the performance of a D_2O laser.

The basic properties of an optically pumped D_2O laser, characterized by a three level system interacting with an FIR and a pump field (Fig. 1), are now well understood in terms of the density matrix formalism [3,4]. In such a system the two photon Raman process plays an important role, as well as the usual two step laser process. Analytical expressions for the gain are obtained, which are functions of pump intensity, FIR intensity and pump frequency off-set. Assuming a steady state level population, the FIR gain for given pump conditions can be calculated. Since in a FIR laser system, both pump and FIR intensities are functions of time, a dynamic simulation model

is necessary to investigate a high power pulsed D_2O laser. As a consequence of axial pumping, the variation of pump intensity along the cavity has to be taken into account. Theoretical studies in the past either did not include spatial effects from a resonator [5] or did not consider off-resonant pumping [6].

In this paper we investigate the performance of a D_2O laser pumped longitudinally by a CO_2 laser. Our approach is based on a coupled rate equation model, in which the two photon process, the bottle neck effect and the decrease in pump intensity due to absorption are all taken into account.

II NUMERICAL MODEL

A. Rate equations

An optically pumped D_2O laser is basically characterized by the three level system shown in Fig. 1. Molecules are pumped from a particular rotational level in the ground vibrational state to a rotational level in the upper vibrational state. FIR laser action then takes place between the pumped rotational level and an adjacent lower lying one. In addition to this two-step laser process, a two-photon Raman process with an appropriate pump off-set is also possible, labeled (2) in Fig. 1. The complete description of these processes is complex. For the case of a single mode FIR laser pumped by a single-mode CO_2 laser, however, analytical gain expressions have been obtained, based on a density matrix formalism [4]. The gain coefficient

G_p for the pump radiation and G_f for the FIR radiation can be expressed by

$$G_p = \sigma_{31} [S_3(n_3 - n_1) - S_4(n_1 - n_2)] \quad (1)$$

$$G_f = \sigma_{32} [S_1(n_3 - n_2) + S_2(n_1 - n_2)] \quad (2)$$

where n_i is the population density of the ith rotational level in Fig. 1 and σ_{ij} is the stimulated emission cross-section on the molecular line centre. The line shape function S_i is a complicated function of pump and FIR intensities, as well as pump and FIR off-sets from the molecular line centre. The analytical form of S_i has been given in ref. [4]. These gain coefficients are divided into two parts: One represents the two-step process which is proportional to $(n_3 - n_1)$ or $(n_3 - n_2)$ and the other the two-photon process which is proportional to $(n_1 - n_2)$.

In an actual laser system, the vibrational decay process plays an important role. Since the vibrational decay constant τ_v is on the order of the pump pulse duration (< 1 μsec) or longer, an intense and long pump pulse depletes the ground vibrational level, whereupon laser action ceases. This bottle neck effect limits the FIR energy extractable from a given FIR laser volume.

Taking the bottle neck effect into account, the set of rate equations for a single-mode D_2O laser pumped by a single-mode CO_2 laser can be written as follows [7].

$$\dot{n}_1 = -(n_1 - f_1 n_g) / \tau_j + I_p G_p \tag{3}$$

$$\dot{n}_2 = -(n_2 - f_2 n_v) / \tau_j + cQG_f \tag{4}$$

$$\dot{n}_3 = -(n_3 - f_3 n_v) / \tau_j - I_p G_p - cQG_f \tag{5}$$

$$\dot{n}_g = I_p G_p - (n_g - f_g n_0) / \tau_v \tag{6}$$

$$n_0 = n_g + n_v \tag{7}$$

$$\dot{Q} = cQG_f - Q/t_c + \dot{Q}_0 \tag{8}$$

where I_p and Q are the pump photon flux and FIR laser photon density in the laser cavity, respectively. τ_j, τ_v and t_c denote the rotational, the vibrational and the cavity lifetime, respectively, and c is the speed of light. The sum of the molecular densities of the ground and the excited vibrational level, $n_g + n_v$ is set to be equal to the total molecular density n_0. Each rotational level tends to be thermalized within a given vibrational level with the Boltzman occupation factor f_i. $\dot{Q}_0$ denotes a spontaneous or a back-ground FIR photon density emission rate and just acts as the seed for the build up of FIR laser radiation. The cavity lifetime t_c consists of two parts, t_ℓ and t_R.

$$1/t_c = \frac{1}{t_\ell} + \frac{1}{t_R}$$

$$1/t_\ell = -\frac{c}{2L} \ln (1 - \alpha) \tag{9}$$

$$1/t_R = -\frac{c}{2L} \ln R_1 R_2$$

where L is the cavity length, R_i the mirror reflectivity and α the single pass loss, which comes from diffraction, scattering or imperfect optical elements.

The available FIR output power P_{out} is given by

$$P_{out} = \frac{h\nu_f}{t_R} Q \qquad (10)$$

where $h\nu_f$ is the energy of a single FIR photon.

B. Pumping geometry

The rate equations (3) - (8) do not contain any spatial variation. The assumption of a constant FIR intensity within the resonator is reasonable, since the sum of the counter propagating FIR beams is indeed almost constant. In order to take into account the influence of the absorption of pump radiation, the pump photon flux I_p was approximated by the pump photon flux I_{av} averaged over the cavity length.

In Fig. 2, we show schematically the most frequently used pumping geometry and the variation of the pump intensity along the cavity. The FIR lasers cavity is formed between the two mirrors M_1 and M_2. FIR lasers are usually pumped longitudinally and the cavity length is fairly long, typically 3-4 m. In our code we include a section between the entrance window W of the FIR tank and the mirror (or mesh) M_1. This section, labeled I in Fig. 2, also contains the FIR active medium, hence it absorbs CO_2 radiation but does not form part of the resonator. For the region I of length ℓ and II of length L, the averaged photon flux I_{pav} is given by

$$I_p^{av} = I_0 \, (e^{G_p \ell} - 1)/G_p \ell \quad \text{for region I}$$

$$I_p^{av} = I_\ell \, (e^{G_p L} - 1)/G_p L \quad \text{for region II} \tag{11}$$

and

$$I_\ell = \gamma I_0 e^{G_p \ell}$$

G_p is a function of pump intensity and FIR intensity, as well as time and therefore G_p was calculated in each integration step. I_0 is the input and I_ℓ the transmitted pump power of the region I, and both are used to calculate G_p for the regions I and II. The element M_1 acts as a reflector in the far infrared and has a transmission of γ for the pump radiation.

The transmission of the region I was calculated as a function of time, by setting Q = 0 in eqs. (3)-(7). Then the full rate equations (3)-(8) were solved for the region II, using the reduced pump intensity transmitted through the region I.

The input pump flux I_0 is approximated by the following function:

$$I_0 = \frac{4}{\pi D^2} \frac{E_0}{h\nu_f t_p} \frac{t}{t_p} e^{-t/t_p} \tag{12}$$

where E_0 is the total pump energy, D the diameter of the pump beam and t_p the time when the pump power reaches the peak value. The total FIR output energy E_{out} is obtained by

$$E_{out} = \frac{\pi}{4} D^2 L \frac{h\nu_f}{t_R} \int Q dt \tag{13}$$

In the following results, the Raman resonance condition is always assumed. This is justified, because it has been observed that the FIR laser frequency changes with the off-set of the pump frequency in a pulsed D_2O laser pumped with a single mode CO_2 laser [8]. The rate equations were solved by the Runge-Kutta method, using the numerical constants listed in Table I which are typical for a D_2O laser at 385 μm. One molecular constant in table I, the vibrational decay constant τ_V, which is the most important constant for high-power, long-pulse operation of FIR lasers, is not well known, but it is estimated to be around 1 μsec [9]. This comparatively fast self-deactivation of the excited vibrational level is possible as a result of fast inter-vibrational decay processes [10]. Some of the other constants were fitted to our experimental conditions [11].

III. RESULTS AND DISCUSSION

A. Pressure dependence of output energy

Fig. 3 shows the calculated FIR output energy as a function of D_2O pressure for different pump energies and cavity lengths. These curves show the familiar pressure dependence of D_2O lasers. In a longitudinally pumped D_2O laser, the optimum pressure which gives maximum output energy is mainly determined by the absorption property of the D_2O cell and by pressure broadening at high pressure. Fig. 4 shows the calculated transmission through a D_2O cell as a function of D_2O pressure neglecting the presence of FIR radiation. From Fig. 3-4

it is clear that on the low pressure side the decrease of output energy is due to less absorption. Maximum output energy is obtained at a pressure for which 80 - 90 % of the pump energy is absorbed.

On the high pressure side, the decrease of output energy is due to the increase in the molecular collision rate, which leads to broadening and decrease of the gain profile. Two other mechanims also contribute to the reduction of output energy at high D_2O pressures: (1) only a short part of the cavity is well pumped and (2) the effective pump energy is lower than that at low pressure operation due to the absorption in region I (Fig. 2). In some cases (high pressure) the output energy is considerably improved by reducing the length of the lossy section between the entrance window and the mirror M_1 (Fig. 2). Around the optimum pressure, however, the influence of the 35 cm long absorbing path is not very important. With this behaviour of the absorption of the pump beam, the operational characteristics of a longitudinally pumped FIR laser can basically be explained, as can be seen in the following results.

The optimum pressure slightly depends on the conditions of operation. For a short cavity a higher pressure is required to efficiently absorb the pump beam. With increasing pump intensity, the D_2O cell becomes transparent due to the usual saturation and/or bottleneck effect. Thus, the optimum pressure is shifted toward the high pressure side by shortening the cavity length and by increasing the pump intensity.

B. Bottle neck effect

When the working pressure is varied, we also observe a change in the shape of the FIR laser pulse. Fig. 5 shows the profiles of the FIR laser pulse as well as the incident and the transmitted CO_2 pump pulse. In a strongly pumped cavity at low pressure (1 torr), where the vibrational decay time is long, the bottleneck effect plays an important role. As a result the FIR pulse duration is shortened. The behaviour of the transmitted CO_2 pulse is typical for a Raman process: the pump beam is strongly absorbed during FIR laser operation due to the fact that emission and absorption are coupled in a two-photon process. Around the optimum pressure of 3 Torr, the FIR pulse roughly follows the pump pulse shape, producing the maximum pulse duration. For further increase of the working pressure, the pulse shape is not affected by the bottle neck effect but by excess absorption. The onset of the FIR pulse is delayed with increasing working pressure mainly because the leading section I (Fig. 2) has to be bleached before efficient pumping of the resonator occurs.

Fig. 6 shows the FIR output energy as a function of pump energy for the two different D_2O pressures of 2 and 5 Torr. For each D_2O pressure the vibrational decay time has been varied between 1 μs torr and 10 μsec torr to demonstrate its influence on the saturation behaviour. This is in good qualitative agreement with experimental results from our laser system [11].

In order to avoid pump saturation, it will be necessary to increase the relaxation rate from the excited ν_2 vibrational level of

D_2O to the ground state. This can be achieved by adding a suitable buffer gas, as has already been demonstrated for cw FIR laser systems [12].

For a mixture of D_2O with a buffer gas M the effective rotational and vibrational relaxation times $\tau_{R,eff}$ and $\tau_{V,eff}$ consist of two components describing collisions between D_2O - D_2O and D_2O - M. They depend on the partial pressures p_{D_2O} and p_M of the two species in the following way

$$\tau_{i,eff} = (p_{D_2O} + p_M)\,(p_{D_2O}/\tau_{i,\,D_2O} + p_M/\tau_{i,M})^{-1} \qquad i = R,V \qquad (14)$$

Collisions between buffer gas molecules are irrelevant in this context. In general, both vibrational and rotational relaxation rates will be affected by collisions between molecules. Whereas an increase in the vibrational relaxation rate will lead to higher FIR output energies, a simultaneous increase in rotational relaxation will have a negative effect. The net effect for a given molecule is a function of both partial pressures as shown in Fig. 7. If $\tau_{V,eff}$ due to the buffer gas is small, an improvement is to be expected mainly at low pressures. On the other hand if $\tau_{R,eff}$ is small, the output energy will be reduced especially for high pressure operation. As a consequence there is an optimum partial pressure of the buffer gas.

For the selection of an optimum buffer gas the following criteria can be derived from these studies: it should absorb neither the pump nor the FIR radiation and while considerably improving the vibrational

relaxation of the ν_2 level of D_2O, it should have a negligible influence on the rotational relaxation. In another paper [11] we report on experimental results using SF_6 as a buffer gas. Fitting these measurements with our theory we obtain $\tau_{V,M} \approx 4$ μsec torr and $\tau_{R,M} \approx 20$ nsec. While these are reasonable values they can, however, only be considered as coarse estimates.

C. Design Parameters

As can be seen above, the operational characteristics are largely affected by the working pressure. Fortunately, during experimental studies the working pressure is the most easily adjustable parameter to maximize the output energy. From the practical point of view, therefore, it is more profitable to simulate other design parameters, such as the pump energy density, the reflectivity of the output coupler and the pump off-set, for a given CO_2 pump laser system, since they usually have to be chosen at the onset and are not easily changed.

Fig. 8 shows the FIR laser efficiency (FIR output energy divided by pump energy) as a function of pump energy density for several pump pulse durations from 0.1 μsec to 1.2 μsec. For a given pump pulse duration there is an optimum pump energy density which changes from $\sim$ 0.35 J/cm^2 for a pump pulse duration of 0.1 μsec to $\sim$ 1 J/cm^2 for a pump pulse duration of 1.2 μsec at 5 torr of D_2O pressure. Although the absolute figures will depend on the exact vibrational relaxation time, these calculations can be used to estimate the

decrease in efficiency when the pump pulse duration is increased. As an example, the efficiency for a 0.1 μsec pump pulse is twice that of a 1.2 μsec pump pulse. These results give the optimum pump beam diameter for a given CO_2 pump energy.

Fig. 9 shows the FIR output energy as a function of the reflectivity of the output coupler. Since FIR lasers have a very high small signal gain, typically more than 10 %/cm, the optimum mirror reflectivity is low. In Fig. 9, the FIR output energy decreases monotonically with increasing reflectivity of the output coupler. In addition, the ratio of the output energy for high intracavity losses to that for low losses is sensitively dependent on the mirror reflectivity and decreases rapidly with increasing reflectivity. These losses are due to diffraction and the imperfections of the coupling mirror M_2 in Fig 2.

Another parameter of an optically pumped D_2O laser which may be optimized is the frequency difference between the pump line and the absorption transition. Fig. 10 shows the FIR output energy and the efficiency as a function of pump off-set. In these calculations, the dependence of the CO_2 laser pump energy on frequency is assumed to be the following function:

$$E(f) = E_0 \cos(0.4\ (f + 0.32)) \qquad (15)$$

which is obtained from a fit to experimental data [13]. Here, f is the pump off-set from the D_2O line centre in GHz, and E_0 is the maximum pump energy at the CO_2 line centre. The CO_2 tuning curve used is also shown in Fig. 10. As expected from the theory [3], off-line centre

pumping is more efficient than resonant pumping. Already, the natural off-set of -320 MHz between D_2O line centre and CO_2 line centre gives reasonable improvement in FIR output energy. The results of Fig. 10 show good agreement with experimental observations [13]. In Fig. 10, tuned pumping is limited by the tunability of the CO_2 pump laser. Fig. 11 shows a similar graph to Fig. 10 for a tuned pump with constant pump energy as might be obtained with a multi-atmosphere pump laser. The FIR output energy varies rather slowly around the optimum pump off-set and we see that the increase in the output energy due to the improved tunability of the pump laser is not very significant.

In general, a comparison of the results from our numerical simulation with experimental measurements shows good qualitative agreement. However, the calculated output energies are a few times higher than those achieved during experiments in our laboratory [11] as well as by other authors [13,14]. One or more of the following reasons could be responsible for this discrepancy: (1) The uncertainty in the vibrational decay time. More detailed information about the molecular relaxation processes and a modification of the set of rate equations are necessary if effects like self-deactivation by inter-vibrational collisions have to be taken into account. (2) The influence of the transverse mode structure. Especially in an unstable resonator, this causes a time varying reflectivity of the output coupler [15]. (3) The transverse imhomogeneity of the pump beam in experiments. This could cause a large diffraction loss. (4) The residual absorption due to the rotational transition within the ground vibrational state, such as $4_{-4} \rightarrow 4_{-2}$ which is only 3.7 GHz different from the 385 µm line centre with a line centre absorption coefficient of 0.45 cm^{-1} [7].

IV. CONCLUSION

Numerical studies of an optically pumped D_2O laser, using a spatially averaged time resolved simulation code, are presented. Pressure dependence of the output energy, saturation behaviour, off-resonance pumping as well as the vibrational "bottle neck" effect have been investigated. From the results we conclude that for longitudinal pumping the performance of a high power D_2O laser strongly depends on the efficiency of pump beam absorption. This has to be considered with regard to optimisation of a D_2O laser towards higher output energies.

This work has been supported by the Ecole Polytechnique Fédérale de Lausanne, the Swiss National Science Foundation and by EURATOM.
One of the authors, T. Okada, would like to thank Prof. K. Muraoka for his continuous encouragement throughout the work.

REFERENCES

[1] M.R. Green, P.D. Morgan, M.R. Siegrist, and R.L. Watterson; A study of the Feasibility of Measuring the Plasma Ion Temperature in JET by Thomson Scattering Using a Far-Infrared Laser, CRPP, LRP 168/80 (1980).

[2] T. Okada, K. Kato, R. Noudomi, K. Muraoka, and M. Akazaki; Plasma Physics 23 (1982) (to be published)

[3] R.L. Panock and R.J. Temkin; IEEE J. Quantum Electron., QE-13 (1977) 425-434

[4] T.A. DeTemple, Infrared and Millimeter Waves (edited by K.J. Button), Vol. 1, Ch. 3, Academic Press, New York

[5] R.J. Temkin and D.R. Cohn, Opt. Commun., 16 (1976) 213-217

[6] M.R. Siegrist, M.R. Green, P.D. Morgan, I. Kjelberg, and R.L. Watterson, J. Appl. Phys. 51 (1980) 3531-3535

[7] S.J. Petuchowski, A.T. Rosenberger, and T.A. DeTemple, IEEE J. Quantum Electron., QE-13 (1977) 476-481

[8] H.R. Fetterman, P.E. Tannenwald, C.D. Parker, J. Helngailis, R.C. Williamson, P. Woskoboinikow, H.C. Praddaude, and W.J. Mulligan, J. Appl. Phys., 34 (1979) 123-125

[9] R.L. Sheffield, K. Boyer, and A. Javan, Opt. Lett. 5 (1980) 10-11

[10] E. Weitz and G.W. Flynn, J. Chem. Phys. 58 (1973) 2781-2793

[11] R. Behn, I. Kjelberg, P.D. Morgan, T. Okada, M.R. Siegrist, Appl. Phys.

[12] T.Y. Chang, C. Lin, J. Opt. Soc. Am. 66 (4) (1976) 362

[13] P. Woskoboinikow, H.C. Praddaude, W.J. Mulligan, D.R. Cohn, and B. Lax, J. Appl. Phys., 50 (1979) 1125-1127

[14] L.C. Johnson and A. Semet, Presented at 5th International Conference on Infrared and Millimeter Waves

[15] M.R. Siegrist, M.R. Green, P.D. Morgan, and R.L. Watterson, Appl. Opt., 19 (1980) 3824-3829

FIGURES CAPTIONS

Fig. 1 : Schematic energy level diagram of an optically pumped D_2O laser. (1) two step laser process, (2) two photon Raman Process. N_i are population densities and τ_v, τ_j the vibrational and rotational relaxation time constant, resp.

Fig. 2 : The pumping geometry used in the numerical model. The FIR cavity is formed by the mirrors M_1 and M_2. M_1 transmits the pump beam with a transmission coefficient of γ. The section I between mirror M_1 and the input window W does not contribute to the FIR output but absorbs pump radiation.

Fig. 3 : The FIR output energy as a function of D_2O pressure for different pump energies and cavity lengths.

Fig. 4 : The transmission of a D_2O cell at the pump line as function of D_2O pressure.

Fig. 5 : Temporal pulse shapes of the FIR output and the CO_2 radiation transmitted through the cell for different D_2O vapour pressures. The input pump pulse is shown in (a).

Fig. 6 : The FIR output energy as function of pump energy for two vapour pressures and 3 vibrational decay constants.

Fig. 7 : The calculated FIR output energy as function of buffer gas pressure for different vibrational and rotational decay constants and D_2O pressures. The pairs of numbers in brackets are $\tau_{V,M}$ in μsec torr and $\tau_{R,M}$ in nsec torr. (L = 2m, D = 11cm, t_p = 400 nsec, pump energy = 100 J)

Fig. 8 : The FIR laser efficiency as function of pump energy density for different pump pulse durations.

Fig. 9 : The FIR output energy as a function of the reflectivity of the output coupler for different intracavity losses.

Fig.10 : The FIR output energy (a) and the FIR laser efficiency (b) as function of the pump frequency off-set, for the CO_2 laser efficiency shown in (c).

Fig.11 : Similar to Fig. 10 but for a frequency independant pump source.

TABLE I : Numerical constants used in the calculation

σ_{13} : 6.7×10^{-16} cm^2 torr	R_1 : 1.0
σ_{23} : 7.4×10^{-15} cm^2 torr	R_2* : 0.1
τ_j : 8 nsec torr	L* : 400 cm
τ_v* : 5 μsec torr	ℓ : 35 cm
f_1 : 0.018	D : 14 cm
f_2 : 0.028	t_p* : 450 nsec**
f_3 : 0.025	α* : 0.5
f_v : 0.005	γ : 0.9
f_g : 0.995	

* These values are used as variable parameters. When values different from those in this table were used, this is indicated in the appropriate figure.

** This value corresponds to a pulse duration (FWHM) of about 1.2 μsec.

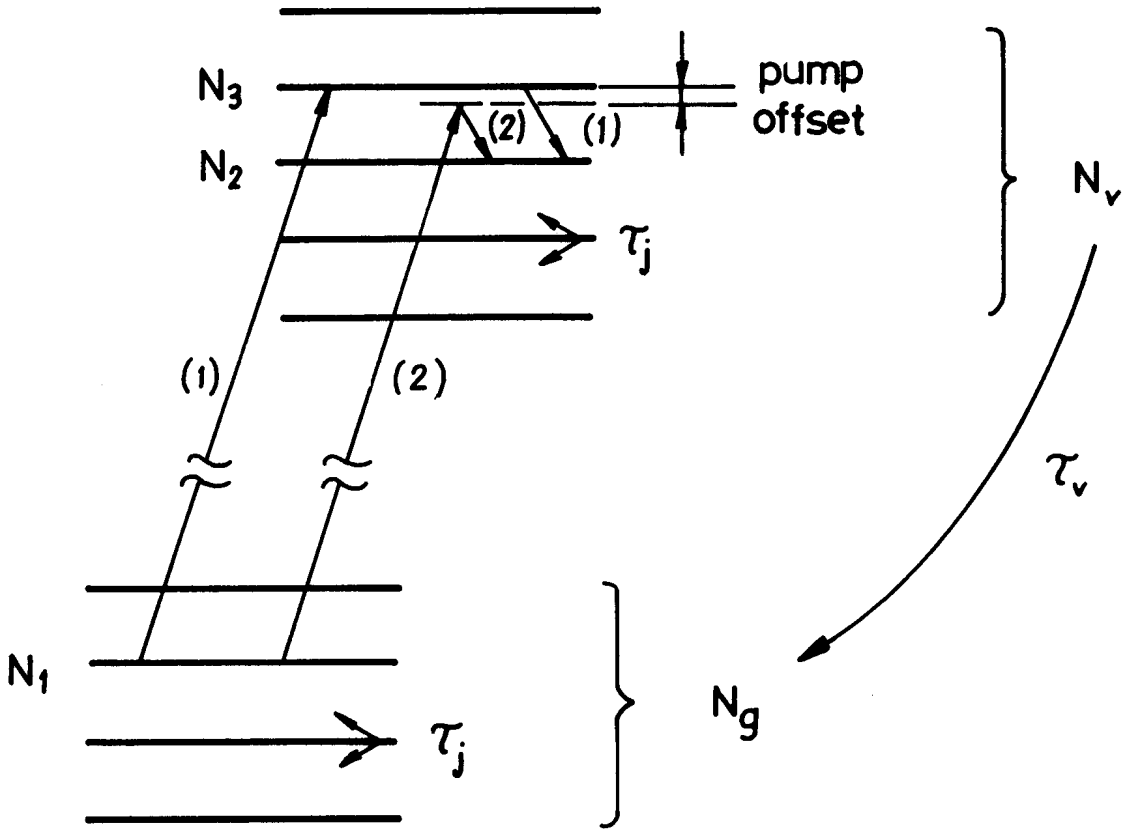

fig. 1

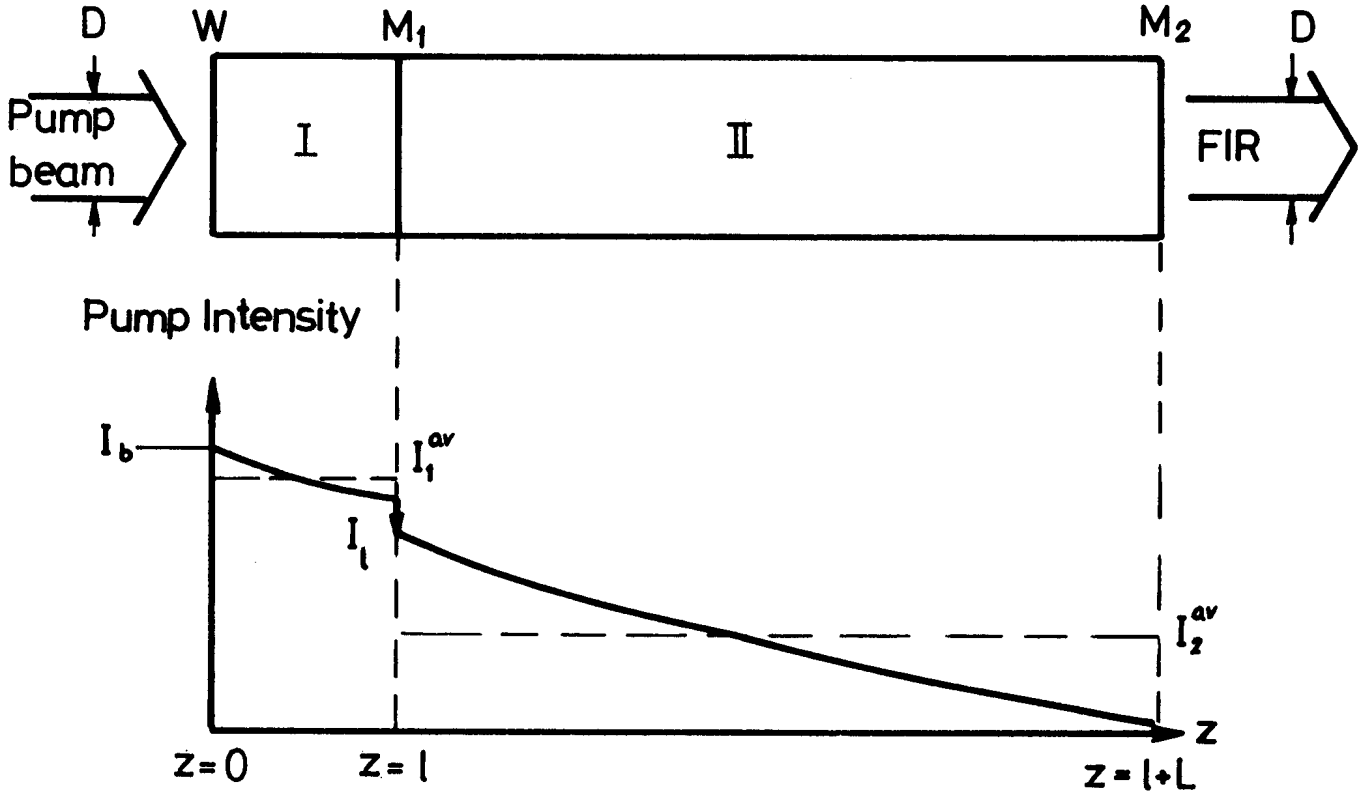
D
W
M1
M2
D
Pump
beam
I
II
FIR
Pump Intensity
Ib
I1av
Il
I2av
z
z=0
z=l
z=l+L

fig.2